1 **Morphological and chemical evidence for cyclic bone growth in a fossil hyaena**

2

3 Jennifer Anné[*1,2], Roy A. Wogelius[1,3], Nicholas P. Edwards[1,4], Arjen van Veelen[2,5], Michael

4 Buckley[1],William I. Sellers[1], Uwe Bergmann[4], Dimosthenis Sokaras[4], Roberto Alonso-Mori[4],

5 Virginia L. Harvey[1], Victoria M. Egerton[1,2], Phillip L. Manning[1]

6

7 [1]University of Manchester, School of Earth and Environmental Sciences, Interdisciplinary Centre for

8 Ancient Life, Manchester M13 9PL, UK

9 [2]The Children's Museum of Indianapolis, Indianapolis, IN, 46206, USA

10 [3]University of Manchester, School of Earth and Environmental Sciences, Williamson Research Centre

11 for Molecular Environmental Science, Manchester M13 9PL, UK

12 [4]SLAC National Accelerator Laboratory, Menlo Park, CA, 94025, USA

13 [5]University of Southampton, Faculty of Engineering and the Environment, Southampton, SO17 1BJ,

14 UK

15

16 **1. Hyaena Specimens**

17 Extant hyaena specimens consist of four adult *C. crocuta* ribs from the collections of the American

18 Museum of Natural History (AMNH; fig S1). Individuals were selected based on their collection in

19 the wild (Kenya and Tanzania) as captive animals are less likely to develop zonal tissue due to

20 constant conditions provided in captive environments. Specimens represent both males (83953 and

21 187769) and females (114226 and 114227).

22

23 Fossil hyaena consists of three isolated elements of *C. c. speala* from the Creswell Crags (UK),

24 currently housed at the Manchester Museum (Manchester, UK; fig S2). Elements include a partial

25 radius (LL.20879), metacarpal (LL.2200) and isolated bone fragment (P.3062). P.3062 was identified

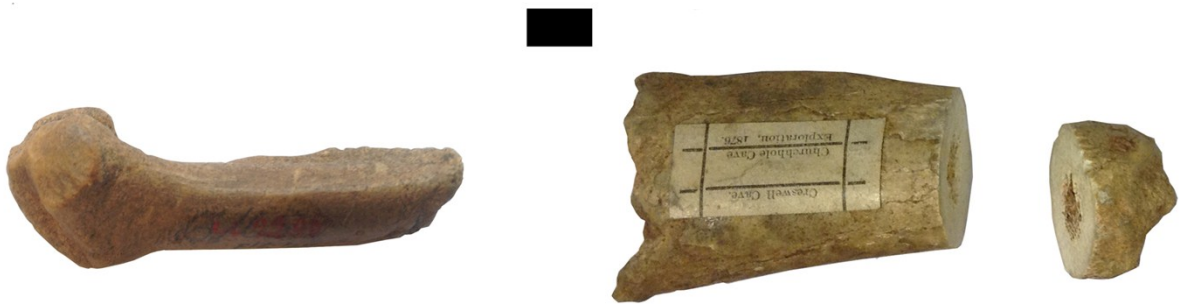26 as hyaena using protein fingerprinting (see section 3).

187769   83593   ▬   114226   114227

Figure S1: Extant hyaena specimens used in this study. Scale bar is 1 cm.


LL.20879

LL.2200   P.3062

Figure S2: Fossil hyaena used in this study. Scale bar is 1 cm.

2. Fossil Location

Creswell Crags is part of the Southern Magnesian Limestone that runs from near Tynemouth to Nottingham (UK; fig S3)[1-2]. Rock types consist of Upper Permian deposits of oolitic to dolomitic limestones, with caves forming from either hydrological dissolution or from rift-slip and fissure formation. These caves vary in age from 50 to 10 ka, with changes in floral and faunal assemblages representing ice age cycles. The specimens in this study are from Pin Hole (38.7 ka) and Church Hole (26.84 to 24 ka) caves[1]. Both Pin Hole and Church Hole cave were first excavated in 1875 and have been interpreted as having similar occupation histories of Neanderthals followed by hyaena and then humans. Evidence for Neanderthals and humans is seen in various stone tools and some fragmentary skeletal material. Evidence for use of these caves as hyaena dens comes from the large mass of fragmentary and gnawed bone[1-2].
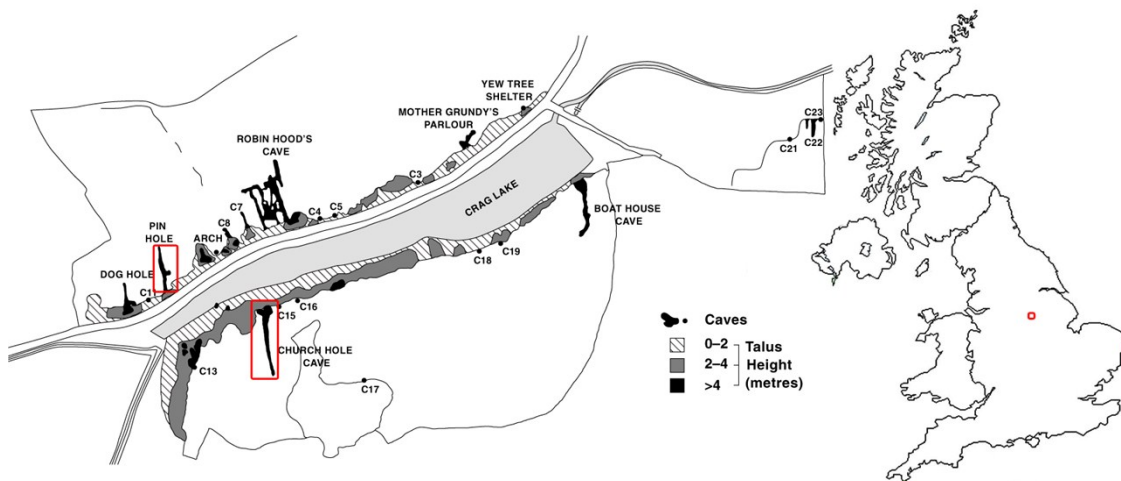
Figure S3: Creswell Crags gorge. Map of the Creswell Crags gorge with caves and fissures labelled and Pin Hole and Church Hole caves highlighted[2]. The location of Creswell in relationship to the UK is marked in red.

3. Protein Fingerprinting

A collagen peptide mass fingerprint was acquired following the methods of [3] (fig S4). In brief, ~50 mg bone sample was demineralised with 1 mL 0.6 M hydrochloric acid (HCl) and ultrafiltered into 50 mM ammonium bicarbonate using a 10 kDa molecular weight cut-off membrane. A 100 uL retentate was removed and digested with 0.2 ug sequencing grade trypsin (Promega, UK) at 37ºC for 18 hours. The peptides were then purified by C18 ziptipping (OMIX), evaporated and resuspended with 10 uL 0.1% trifluoroacetic acid. 1 uL of this solution was then spotted onto a stainless steel target plate and co-crystalised with 1 uL 10 mg/mL alpha-cyano hydroxycinnamic acid and, following calibration, analysed on a Bruker Ultraflex II Matrix Assisted Laser Desorption Ionization Time of Flight mass spectrometer with 10,000 laser acquisitions. The fingerprint was then compared with taxonomic markers presented by [4-5].
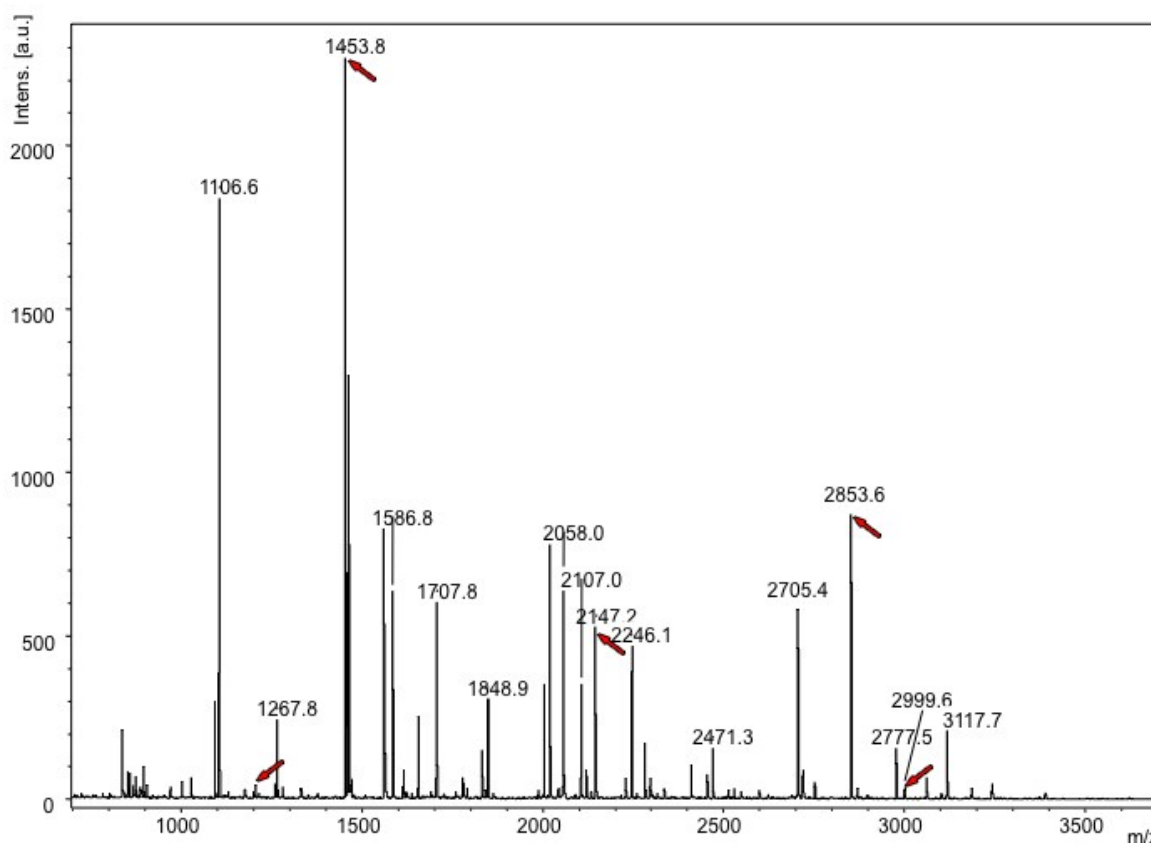
Figure S4: Peptide mass fingerprint. Peptide map fingerprint of collagen confirming identification of bone specimen P.3062 as hyaena (markers indicated matching to peptide markers in [5]).

4. Synchrotron Elemental Mapping

SRS-XRF (SSRL): Maps were collected with an incident beam energy of 13.5 keV for heavier elements (high-*Z*; Ca and higher) and 3.15 KeV for lighter elements (low-*Z*; Ca and lower). For maps of high atomic number elements (Ca-As), the specimen is aligned at a fixed incident angle of 45° relative to the incident beam with a single element drift detector (Vortex) set at 90° scattering angle to the incident beam. For maps of low atomic number elements (S-Cl), the specimen is placed in a helium-purged sample chamber and the scattering angle was changed to ~160° to minimize signal loss. Element windows are manually set by collecting a raw Energy-Dispersive X-ray Spectrum (EDS) from an area of the map containing the majority of the different materials present in the sample (e.g. matrix, hard tissue, soft tissue; fig S5).

Microfocus Mapping (Diamond Light Source)**:** The sample was mounted on an x-y-z stage and rastered at a 45° angle to the incident X-ray beam with a four element Si drift detector Vortex fluorescence detector set at 90° scattering angle. Windows were assigned to the detector post data collection as a full spectrum is collected for each pixel. Maps were processed using the ROI tool in PyMCA[6], which are then used to determine areas for the single energy dispersive spectra (EDS). To make a map using the ROI imaging tool, an energy range is selected around a peak in the EDS

80　spectra. The ROI image then displays the distribution of the energy selected rather than the full

81　spectra. The peak selected is identified based on the energy using (ex. Zn Kα at 8.64 keV). This step

82　is repeated for every peak identified on the EDS spectra, resulting in maps of all the elements present.

83

84　**5. Quantification from SSRL and Diamond Light Source (DLS) data using PyMCA**

85　To quantify element concentrations, multiple EDS were undertaken by locating an area of interest

86　within the scan, driving the stage to the area, and collecting a full energy spectrum for 50 sec (SSRL)

87　or 30 sec (DLS). Multiple spectra are taken per area of interest to account for chemical variation

88　within the sample. For quantification taken at SSRL, the location of point analyses were chosen using

89　the PointAnalysisHelper software written by co-author William Sellers, which translates pixel

90　locations on RAS maps to motor positions using map coordinates. For DLS, exact motor positions are

91　saved for each pixel, allowing for precise locations to be selected using the viewed elemental maps.

92　Spectra are then processed through the PyMCA software[6], which is used to fit spectra based on the

93　raw EDS files and from the experimental parameters using a Durango apatite standard of known

94　elemental concentrations for calibration.

95
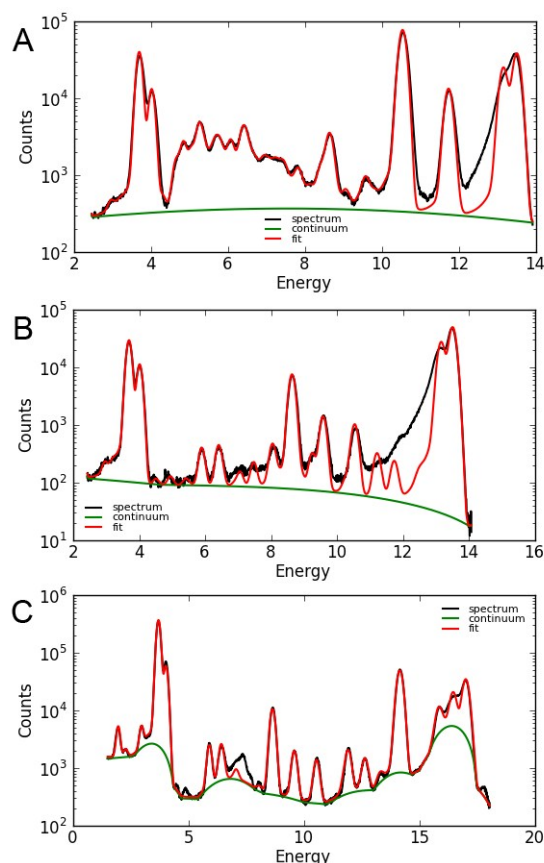
96

97　**Figure S5: EDS spectrum.** Example of EDS spectrum fitted using PyMCA from the Durango standard (A),

98　extant hyaena (B) and fossil hyaena (C).

99

For extant bones, the influence of the organic content within the sample had to be considered in order to calculate elemental concentrations. Although elements associated with organics (H, O, C, N) are too light to be detected by the experimental set up at SSRL and DLS, they do influence the stoichiometry of the sample matrix (10-40%), which is used by the PyMCA software in determining trace element concentrations. The organic constituents were added by calculating the stoichiometry of a collagen-apatite mixture and inputting that value into the matrix configuration in PyMCA for extant specimens. For specimens older than 2×10^4 years more than two-thirds of the organic component has been degraded. Thus organic stoichiometry was not included in our fossil calculations due to the extremely low organic content in the fossil versus the extant bone, which would cause PyMCA to over compensate for organics and skew the results for fossil material.

6. Additional Quantification Results

The following represent EDS analyses for extant and extinct hyaena taken at SSRL using either a 50 μm (extinct) or 25 μm (extant) pinhole.

Element	Durango	114226 Female	114227 Female	83953 Male	187769 Male
P	18.2% (1.43%)	27.61% (1.02%)	20.09% (0.74%)	18.29% (0.76%)	23.41% (0.89%)
Ca	38.08% (2.42%)	38.1% (2.36%)	36.9% (2.29%)	29.04% (1.86%)	34.96% (2.23%)
Ti	1308	170 (30)	135 (25)	106 (20)	85 (18)
Cr	1431	3 (1)	3 (1)	5 (1)	2 (1)
Mn	482	3 (1)	2 (0.4)	2 (0.4)	1 (0.2)
Fe	569 (37)	37 (6)	62 (9)	57 (4)	29 (5)
Ni	61	4 (1)	4 (1)	4 (1)	2 (0.4)
Cu	18	2 (0.3)	2 (0.4)	8 (1)	1 (0.2)
Zn	73 (2)	142 (11)	161 (12)	165 (11)	106 (8)
As	761 (4)	441 (22)	723 (42)	20 (2)	2 (0.3)

Table S1: XRF EDS analysis concentrations taken at the SSRL for different tissue types of extant hyaena given in ppm or weight percent (%).Fit errors are given in parentheses and represent ± two standard deviations.

6.2 Fossil Hyaena

Low-*Z* (lighter than Ca) elemental concentrations for the cave hyaena fragment, P.3062. Cortical bone is less silicified as expected in a more dense bone tissue. High-*Z* concentrations are given in Table 1.

Element	Durango	Medullary Cavity/ Cancellous Bone	Outer Cortex/Cortical Bone
Al	5453 (454)	4739 (432)	3954 (368)
Si	2408 (176)	189 (16)	26
P	18.18% (0.76%)	15.88% (0.69%)	14.77% (0.67%)
S	730 (63)	315 (32)	318 (32)
Cl	5614 (74)	388 (334)	334 (38)

121 Table S2: XRF EDS analysis concentrations taken at DLS for different tissue types of the extinct hyaena bone
122 fragment (P. 3062) given in ppm or weight percent (%).Fit errors are given in parentheses and represent ± two
123 standard deviations.
124

125 **7. Correlation between optical and elemental images**
126 The correlation 1° plugin in ImageJ[7] was used to show that features observed in the optical histology
127 in the fossil specimen (P.3062) could be correlated with specific elemental distributions (fig S6).
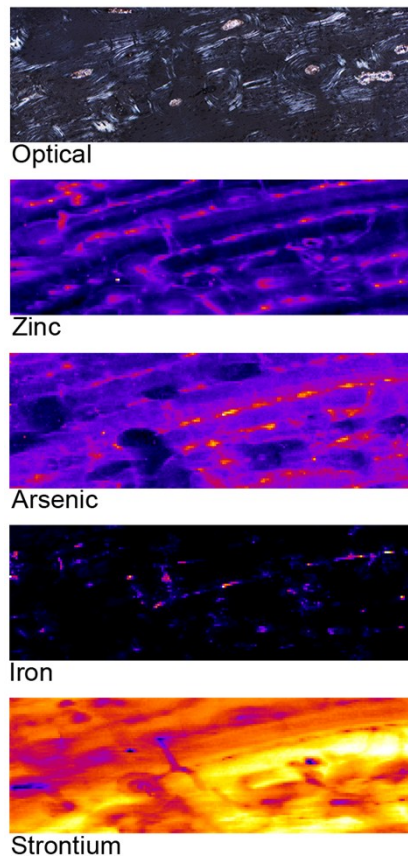
128
129 **Figure S6: Correlation maps.** Maps showing the correlation between histological features seen in optical
130 histology and elemental distributions of Zn, As, Fe and Sr. Hotter colours indicate a stronger correlation.

131 **References**

132   1. Pettit, P., Bahn, P. and Ripoll, S. (eds). 2007. *Paleolithic Cave Art at Creswell Crags in*
133   *European Context*. Oxford University Press, Oxford, UK.

134   2. Hedges, R.E.M, Pettitt, P.B., Bronk-Ramsey, C. and van Klinken, G.J. 1996. Radiocarbon
135   dates from the Oxford AMS system: Arcaheometry datelist 22. *Archaeometry* 38 (2): 391-
136   415.

137   3. van der Sluis, L.G., Hollund, H.I., Buckley, M., De Louwd, P.G.B., Rijsdijke, K.F., Kars, H.
138   2014. Combining histology, stable isotope analysis and ZooMS collagen fingerprinting to
139   investigate the taphonomic history and dietary behaviour of extinct giant tortoises from the
140   Mare aux Songes deposit on Mauritius. *Palaeogeogr. Palaeoclimatol. Palaeoecol.* 416: 80-
141   91.

142   4. Buckley, M. and Collins, M.J. 2011. Collagen survival and its use for species identification in
143   Holocene-lower Pleistocene bone fragments from British archaeological and palaeontological
144   sites. *Antiqua* 1(1): e1.

145   5. Buckley, M., Collins, M., Thomas-Oates, J. and Wilson, J.C. 2009. Species identification by
146   analysis of bone collagen using matrix-assisted laser desorption/ionisation time-of-flight mass
147   spectrometry *Rapid Commun. Mass Spectrom.* 23(23): 3843–3854.

148   6. Solé, V.A., Papillon, E., Cotte, M., Walter, Ph. and Susini, J. 2007. A multiplatform code for
149   the analysis of energy-dispersive X-ray fluorescence spectra. *Spectrochimica Acta Part B:*
150   *Atomic Spectroscopy* 62 (1): 63–68. doi:10.1016/j.sab.2006.12.002.

151   7. Schneider, C. A., Rasband, W. S. and Eliceiri, K.W. 2012 NIH Image to ImageJ: 25 years of
152   image analysis. *Nature methods* 9(7): 671-675.

153